

# Analysis of instabilities and pattern formation in time fractional reaction-diffusion systems\*

B.Y. Datsko<sup>1,†</sup> and V.V. Gafiychuk<sup>1,‡</sup>

<sup>1</sup>*Institute for Applied Problems in Mechanics and Mathematics,  
National Academy of Sciences of Ukraine, Naukova Street 3b, Lviv, Ukraine 79053*  
(Dated: February 13, 2022)

We analyzed conditions for Hopf and Turing instabilities to occur in two-component fractional reaction-diffusion systems. We showed that the eigenvalue spectrum and fractional derivative order mainly determine the type of instability and the dynamics of the system. The results of the linear stability analysis are confirmed by computer simulation of the model with cubic nonlinearity for activator variable and linear dependance for the inhibitor one. It is shown that pattern formation conditions of instability and transient dynamics are different than for a standard system. As a result, more complicated pattern formation dynamics takes place in fractional reaction-diffusion systems.

## I. INTRODUCTION

In reaction-diffusion systems a stable equilibrium solution usually changes spontaneously with parameters to limit cycle by Hopf bifurcation or stationary dissipative structures by Turing bifurcation. As a result, we obtain nonlinear dynamics leading to stationary or oscillatory structures. When conditions of both instabilities arise, we can expect more complex dynamics [1, 2, 3]. In case of a fractional reaction-diffusion (FRD) system dynamics can be much more complex [4, 5, 6, 7, 8, 9, 10, 11, 12].

Last investigation showed that many complex heterogeneous systems are described by differential equations with fractional derivatives to represent their anomalous behavior [13, 14, 15, 16, 17, 18]. Therefore, investigation of pattern formation in FRD system has both theoretical and applied interest.

In this article the FRD system with cubic nonlinearity is studied for the case when both instabilities take place. We have focused on the dynamics of FRD model under conditions when sufficiently complex patterns arise in the system dynamics. The results of analytical treatment of the linearized model are validated by computer simulations of nonlinear dynamics.

## II. MATHEMATICAL MODEL

Let us consider the FRD system

$$\tau {}_c u_t^\alpha = l u_{xx} + W(u, \mathcal{A}), \quad (1)$$

with two variables  $u = (u_1, u_2)^T$  on the  $x \in (0, \mathcal{L})$  subject to Neumann:  $u_x|_{x=0, \mathcal{L}} = 0$  boundary conditions and with certain initial conditions,  $W = (W_1, W_2)^T$ ,  $W_1, W_2$  - smooth reaction kinetics functions,  $\mathcal{A}$  - real

parameter,  $\tau$  and  $l$  are positive diagonal matrices  $\tau = \text{diag}[\tau_i]$ ,  $l = \text{diag}[l_i^2] > 0$ .

Fractional derivatives  ${}_c u_t^\alpha$  on the left hand side of the equations (1), instead of the standard time derivatives, are the Caputo fractional derivatives in time [18, 19] of the order  $0 < \alpha < 2$  and are represented as

$${}_c u_t^\alpha = \frac{\partial_c^\alpha u(t)}{\partial t^\alpha} := \frac{1}{\Gamma(m-\alpha)} \int_0^t \frac{u^{(m)}(\tau)}{(t-\tau)^{\alpha+1-m}} d\tau, \quad (2)$$

where  $m-1 < \alpha < m, m \in \overline{1, 2}$ .

## III. LINEAR STABILITY ANALYSIS

Due to the property of Caputo derivative the stability of the steady-state solutions of the system (1) corresponding to homogeneous equilibrium state  $W(u_0, \mathcal{A}_0) = 0$  can be analyzed by linearization of the system nearby this constant solution  $u_0 = (\bar{u}_1, \bar{u}_2)^T$ . The linearization of FRD system (1) leads to fractional ODEs with right hand side matrix  $F(k) = \begin{pmatrix} (a_{11} - k^2 l_1^2)/\tau_1 & a_{12}/\tau_1 \\ a_{21}/\tau_2 & (a_{22} - k^2 l_2^2)/\tau_2 \end{pmatrix}$ , diagonal form of which is given by eigenvalues  $\lambda_{1,2} = \frac{1}{2}(tr F \pm \sqrt{tr^2 F - 4 \det F})$  (coefficients  $a_{ij}$  represent Jacoby matrix).

For  $\alpha : 0 < \alpha < 2$  for every point inside the parabola  $\det F = tr^2 F/4$ , we can introduce a marginal value  $\alpha : \alpha_0 = \frac{2}{\pi} |Arg(\lambda_i)|$  given by the formula [8, 9]

$$\alpha_0 = \begin{cases} \frac{2}{\pi} \arctan \sqrt{4 \det F / tr^2 F - 1}, & tr F > 0, \\ 2 - \frac{2}{\pi} \arctan \sqrt{4 \det F / tr^2 F - 1}, & tr F < 0. \end{cases} \quad (3)$$

The value of  $\alpha$  is a certain additional bifurcation parameter which switches the stable and unstable states of the system. At lower  $\alpha : \alpha < \alpha_0 = \frac{2}{\pi} |Arg(\lambda_i)|$ , the system has oscillatory modes, but they are stable. Increasing the value of  $\alpha > \alpha_0 = \frac{2}{\pi} |Arg(\lambda_i)|$  leads to oscillatory instability.

\*Preprint submitted to ASME

<sup>†</sup>Electronic address: b'datsko@yahoo.com

<sup>‡</sup>Electronic address: vagaf@yahoo.com

It is widely known for integer time derivatives [1, 2, 3] that system (1) becomes unstable according to either Hopf ( $k = 0$ )

$$\text{tr}F > 0, \quad \det F(0) > 0. \quad (4)$$

or Turing ( $k_0 \neq 0$ ) bifurcations

$$\text{tr}F < 0, \quad \det F(0) > 0, \quad \det F(k_0) < 0. \quad (5)$$

and these both types of instabilities are realized for positive feedback ( $a_{11} > 0$ ) [1, 2, 3].

In the case of fractional derivative index, Hopf bifurcation is not connected with the condition  $a_{11} > 0$  and can hold at a certain value of  $\alpha$  when the fractional derivative index is sufficiently large [10]. Moreover, in fractional RD systems at  $\alpha > 1$  when it is easier to satisfy conditions of Hopf bifurcation, we meet a new type of instability [8, 9]

$$\text{tr}F < 0, \quad 4 \det F(0) < \text{tr}^2 F(0), \quad 4 \det F(k_0) > \text{tr}^2 F(k_0). \quad (6)$$

It is worth to analyze inequalities (6) in detail. Taking into account explicit form of  $F(k)$  the last two conditions can be rewritten as:

$$(a_{11}\tau_1 - a_{22}\tau_2)^2 > -4a_{12}a_{21}\tau_1\tau_2, \quad (7)$$

$$-4a_{12}a_{21}\tau_1\tau_2 > [(a_{11} - k^2 l_1^2)\tau_2 - (a_{22} - k^2 l_2^2)\tau_1]^2. \quad (8)$$

The simplest way to satisfy the last condition is to estimate the optimal value of  $k = k_0$

$$k_0 = 2 \left( \frac{-a_{12}a_{21}}{l_1^2/\tau_2 - l_2^2/\tau_1} \right)^{1/2}. \quad (9)$$

Having obtained (9), we can estimate the marginal value of  $\alpha_0$

$$\alpha_0 = 2 - \frac{2}{\pi} \arctan T, \quad (10)$$

where the expression  $T$  has the following view

$$T = \frac{(-4a_{12}a_{21}\tau_1\tau_2)^{1/2}}{\left| (a_{11}\tau_2 - a_{22}\tau_1) \frac{l_2^2\tau_2 + l_2^2\tau_1}{l_2^2\tau_2 - l_2^2\tau_1} \right| - a_{11}\tau_2 - a_{22}\tau_1}. \quad (11)$$

The analysis of expressions (6) shows that at  $k = 0$  we have two real eigenvalues that are less than zero, and the system is certainly stable for the Hopf bifurcation. If the last inequality takes place for a certain value of  $k_0 \neq 0$ , we can get two complex eigenvalues, and a new type of instability, connected with the interplay between the determinant and the trace of  $F(k)$  of the linearized system, emerges. With such type of eigenvalues, it is possible to determine the value of fractional derivative index when the system becomes unstable for Hopf bifurcation with this wave number [8].

#### IV. FRACTIONAL REACTION DIFFUSION SYSTEM WITH CUBIC NONLINEARITY

To demonstrate the properties of FRD system, let us consider the model with cubic dependence for activator variable  $W_1 = u_1 - u_1^3 - u_2$  and the linear for the inhibitor variable  $W_2 = -u_2 + \beta u_1 + \mathcal{A}$ . This model was proposed firstly by R. FitzHugh [20] for description of the propagation of voltage impulse through a nerve axon and is known as Bonhoeffer-van der Pol model. In RD systems this model was considered in many books and articles (see for example [1, 2, 3]). The homogeneous solution of variables  $\bar{u}_1$  and  $\bar{u}_2$  can be obtained from the system of equations  $W_1(\bar{u}_1, \bar{u}_2) = 0, W_2(\bar{u}_1, \bar{u}_2) = 0$ , which in their turn determine two nullclines  $\bar{u}_2(\bar{u}_1)$ . The intersection of these nullclines in the point  $P = (\bar{u}_1, \bar{u}_2)$  is determined by equation:  $\bar{u}_1 - \bar{u}_1^3 - \beta \bar{u}_1 - \mathcal{A} = 0$ . In this case the values of external parameters  $A, \beta$  determine the value of  $\bar{u}_1$  and this makes it possible to investigate the conditions of different types of instability explicitly considering parameter  $\bar{u}_1$  as the main parameter for system analysis.

For investigation of the Hopf bifurcation let us consider homogeneous perturbation with  $k = 0$ . The linear analysis of the system with  $\alpha = 1$  shows that, if  $\tau_1/\tau_2 > 1$ , the solution corresponding to any intersections of two isoclines is stable. The smaller is the ratio of  $\tau_1/\tau_2$ , the wider is the instability region (solid lines with points on Fig. 1). Formally, at  $\tau_1/\tau_2 \rightarrow 0$ , the instability region for  $\bar{u}_1$  coincides with the interval  $(-1, 1)$  where the null cline  $W(u_1, u_2) = 0$  has its increasing part (Fig. 2b). These results are very widely known in the theory of nonlinear dynamical systems [1, 2, 3].

In the fractional differential equations the conditions of the instability depend on the value of  $\alpha$  and we have to analyze the real and the imaginary parts of the existing complex eigenvalues, especially the equation:

$$4 \det F - \text{tr}^2 F = \frac{4((\beta - 1) + \bar{u}_1^2)}{\tau_1 \tau_2} - \left( \frac{(1 - \bar{u}_1^2)}{\tau_1} - \frac{1}{\tau_2} \right)^2 > 0. \quad (12)$$

In fact, with complex eigenvalues, it is possible to find the corresponding value of  $\alpha$  where the condition  $\alpha > \alpha_0$  is true. Omitting simple calculation, we can write an equation for marginal values of  $\bar{u}_1$

$$\bar{u}_1^4 - 2\left(1 + \frac{\tau_1}{\tau_2}\right)\bar{u}_1^2 + \frac{\tau_1^2}{\tau_2^2} - 2\frac{\tau_1}{\tau_2}(2\beta - 1) + 1 = 0, \quad (13)$$

and solution of this biquadratic equation gives us the domain where the oscillatory instability can arise

$$\bar{u}_1^2 = 1 + \frac{\tau_1}{\tau_2} \pm 2\sqrt{\beta \frac{\tau_1}{\tau_2}}. \quad (14)$$

This expression estimates the maximum and minimum values of  $\bar{u}_1$  where the system can be unstable at marginal value of  $\alpha = \alpha_0 = 2$  as a function of  $\tau_1/\tau_2$  and  $\beta$ .

The typical stability domains for considered FRD system in the coordinates  $(\bar{u}_1, \tau_1/\tau_2)$  for different values of

fractional derivative index  $\alpha$  are presented in Fig.1a-d, where curves corresponding to  $\alpha = 1$  are denoted by more solid lines. This makes it possible to see how other curves  $\alpha \neq 1$  are located with respect to standard system  $\alpha = 1$ . The solid points on both sides denote the interval of maximum instability. For each particular value  $\alpha$  in the region between the corresponding curve and horizontal axis, the system is unstable with wave numbers  $k = 0$ , and outside it is stable. Figures (a) and (b) present the plots for the value of  $\beta = 1.01$ . The left-hand side plot corresponds to  $\alpha < 1$  and the right-hand side plot corresponds to  $\alpha > 1$ . It is easy to see from the plot (a) that if the value of  $\tau_1/\tau_2$  increases (we move along vertical axis) the instability domain decreases ( $\alpha < 1$ ). At  $\tau_1/\tau_2 = 1$  and  $\alpha = 1$  it vanishes completely. The solid point in the middle of each plots corresponds to the case when the system becomes stable for all values of  $\bar{u}_1$ : point (0, 1) in coordinates  $(\bar{u}_1, \tau_1/\tau_2)$ . The situation changes for  $\alpha > 1$ . The system is unstable not only for  $\tau_1/\tau_2 < 1$  but also for  $\tau_1/\tau_2 > 1$ . An increase in  $\alpha$  makes the instability domain much wider with respect to two coordinates  $(\bar{u}_1, \tau_1/\tau_2)$  and we obtain butterfly like domains for  $\alpha > 1$ . This means that with increasing  $\tau_1/\tau_2$  (moving along vertical axis) the system becomes stable in the center and unstable at greater values  $\bar{u}_1$ . In such case the instability domain becomes symmetric along vertical axis with the minimum point at the  $\bar{u}_1 = 0$ . We observe similar behavior for large values of  $\beta$ . Instability domains in Fig. 1c,d are presented for  $\beta = 10$  and show the same trend with respect to  $\alpha$ , but the region for  $\alpha > 1$  is much greater than for  $\beta = 1.01$ . At the same time, for  $\alpha < 1$  and  $\beta = 10$  instability domain shrinks very sharply in comparison to the same domain plot when  $\beta = 1.01$ .

It is possible to obtain solid understanding of the mechanism of the instability from the plot of eigenvalues. Typical instability domains for the same parameters as on Fig. 1a,b for  $k = 0$  are presented on the Fig. 2a. Horizontal lines (i, ii, iii) on the instability domain plot correspond to eigenvalues plots below. Let us analyze each of the possible situations in more detail.

For the case (i) we have sub-domains with real positive, real negative and complex eigenvalues. The easiest way of obtaining instability is realized at  $|\bar{u}_1| < \bar{u}_1^E$  when all the roots are real and positive (Fig. 2a(i)). This region is presented by dark grey color and positive eigenvalues mean that the system is unstable practically for any value of  $\alpha > 0$ . Inside the domain  $|\bar{u}_1^E| < |\bar{u}_1| < |\bar{u}_1^C|$  there is a certain domain of  $\alpha$ : ( $0 < \alpha < 2$ ) where the Hopf bifurcation takes place. Point  $D$  divides the region into two domains where  $\text{Re}\lambda < 0$  and  $\text{Re}\lambda > 0$ . In the domain  $\text{Re}\lambda < 0$  the system could be unstable according to greater values of  $\alpha > 1$ . In turn, for  $\text{Re}\lambda > 0$ , the system could be stable at  $\alpha < 1$ . In other words, between points  $C$  and  $E$  we have eigenvalues with imaginary part, and the value of  $\alpha$  can change the stability of the FRD system. In the domain  $|\bar{u}_1| > |\bar{u}_1^C|$  we have two real and negative roots and, as a result, the system is stable.

For system parameters corresponding to the case (ii)

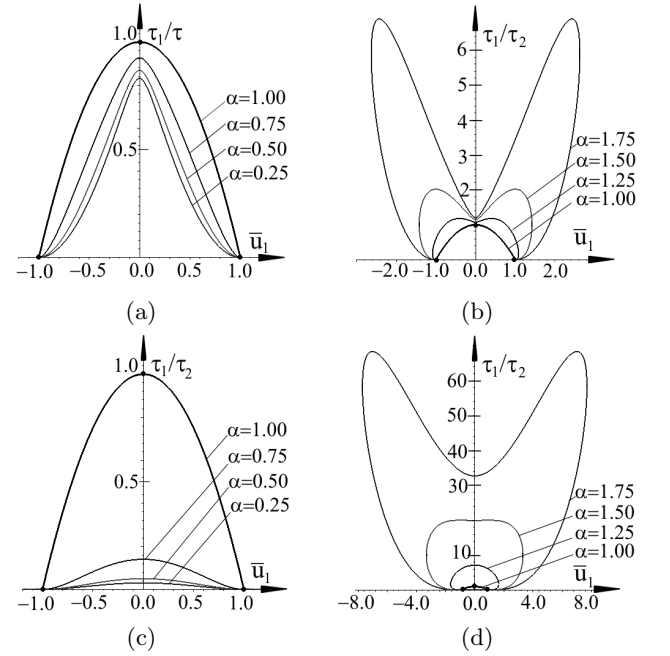


FIG. 1: Instability domains in coordinates  $(\bar{u}_1, \tau_1/\tau_2)$  for a fractional order reaction-diffusion system with sources  $W_1 = u_1 - u_1^3 - u_2$ ,  $W_2 = -u_2 + \beta u_1 + \mathcal{A}$  for different values of  $\alpha_0 = 0.25, 0.5, 0.75, 1.0, 1.25, 1.5, 1.75$ . The results of computer simulation obtained at  $l_1 = l_2 = 0$  for:  $\beta = 1.01$  - (a), (b) and  $\beta = 10.0$  - (c), (d) .

the real part of eigenvalues becomes less than zero for all  $\bar{u}_1$ . At the same time, for  $|\bar{u}_1| < |\bar{u}_1^K|$  the roots are complex and according to condition (3) instability takes place for  $\alpha > \alpha_0 > 1$ . For  $|\bar{u}_1| > |\bar{u}_1^K|$  the roots become real and negative, and the system is stable.

In the case (iii) at the center of  $\bar{u}_1$  ( $|\bar{u}_1| < |\bar{u}_1^G|$ ) we have two real negative eigenvalues, and the system is stable. For  $|\bar{u}_1^G| < |\bar{u}_1| < |\bar{u}_1^H|$  we have complex roots and certainly according to condition (3) instability takes place for  $\alpha > \alpha_0 > 1$ . In this case, the instability domain consists of two symmetrical regions separated by a stable region at the center where the system is stable for any  $\alpha$ . For  $|\bar{u}_1| > |\bar{u}_1^H|$  the system is stable again.

Let us analyze the Turing Bifurcation ( $k \neq 0$ ). Eigenvalues for different values of  $k$  are presented in Fig. 2b. The top plot corresponds to nullclines of the systems just to show that nullcline intersection determines eigenvalues in Fig. 2b(iv). We present eigenvalues for  $k = 1$  and  $k = 2$  and for comparison  $k = 0$ . It can be seen from the picture (iv) that at intersection of nullclines in the vicinity of zero value of  $\bar{u}_1$  nonhomogeneous modes have much greater values and we can expect a formation of stationary dissipative structures. If the ratio  $l_1/l_2$  is sufficiently small, Turing bifurcation is dominant for all region  $\bar{u}_1 < 1$ . Analyzing (5) we can conclude that these conditions are practically the same for fractional and standard RD systems. However, what is very im-

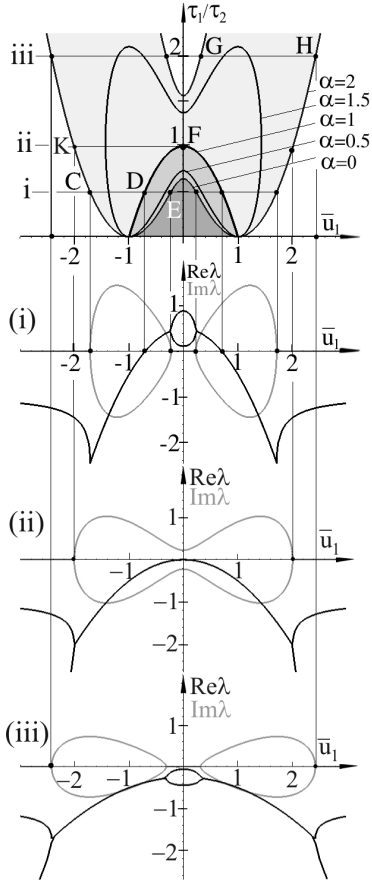


FIG. 2: Instability domains ( $Re\lambda$  - black lines,  $Im\lambda$  - grey lines) for  $k = 0$ ,  $\beta = 1.05$  and different proportions of  $\tau_1/\tau_2 = 0.5$  - (i),  $1.0$  - (ii),  $2.0$  - (iii).

portant is that the transient processes and the dynamics of these systems are different, and for this reason final attractors can often be different even though the linear conditions of instability look the same.

Now let us consider that the system parameters are close to the ones represented by point  $P$  in Fig. 2b. As a result, for certain ratio of  $Im\lambda$  and  $Re\lambda$  we expect the formation of oscillatory inhomogeneous structures. However, if the solution  $\bar{u}_1$  is close to zero, the decrease of  $\alpha$  leads to steady state dissipative structures. Such trend is quite general and if in standard system we have steady state solutions, the increase of  $\alpha$  in FRD system leads to non stationary structures. In this case, by changing intersection point of nullclines or value of  $\alpha$  we can stimulate stationary or temporary pattern formation. If the absolute value of eigenvalues for  $k = 0$  and  $k \neq 0$  are comparable we can expect more complex spatio-temporal dynamics.

Above we have considered that the linearized system is unstable for either Hopf or Turing bifurcation. Below, we consider the case when we don't have Turing or Hopf bifurcation. For realization of instability conditions (6)

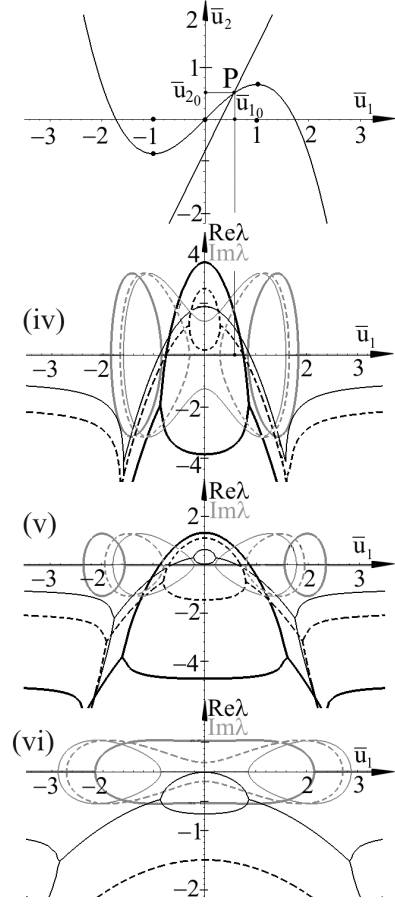


FIG. 3: The null-clines for  $\beta = 2.1$ ,  $A = 0.5$  and eigenvalues for different values of  $k$  ( $k = 0$  - hair-lines,  $k = 1$  - dash lines,  $k = 2$  - thick lines) - (b). The eigenvalues are presented for the following parameters:  $l_1 = 0.025$ ,  $\beta = 2.1$ ,  $\tau_1/\tau_2 = 0.21$  - (iv),  $l_1 = 0.1$ ,  $\beta = 1.01$ ,  $\tau_1/\tau_2 = 0.6$  - (v),  $l_1 = 2.1$ ,  $\beta = 1.01$ ,  $\tau_1/\tau_2 = 3.5$  - (vi).

for  $k \neq 0$ ,  $Im\lambda \neq 0$  the fractional derivative index must be greater than some critical value  $\alpha_0$ . Eigenvalues for such instability are presented in Fig. 2b(v,vi). We can see that outside a small domain in the center the system is stable for  $k = 0$ . At the same time on this interval we have complex eigenvalues for  $k \neq 0$  (Fig. 2b (v)). In the plot (v) for  $l_1/l_2 < 1$  we have a separate domain for  $k = 2$  where we can expect inhomogeneous oscillations with this wave number.

In Figure (vi) we present the situation where all roots have  $Re\lambda < 0$  and in standard system we do not have instability at any values of  $\bar{u}_1$ . In FRD system the roots are complex for select values of  $k$  ( $k \neq 0$ ). In other words, for such system at  $\alpha > 1$  we can obtain conditions of Hopf bifurcation (6) which lead to inhomogeneous oscillatory structures [8, 9] even for  $l_1/l_2 > 2$ . This situation can be predicted from symmetrical view of expression (11) for the system under consideration

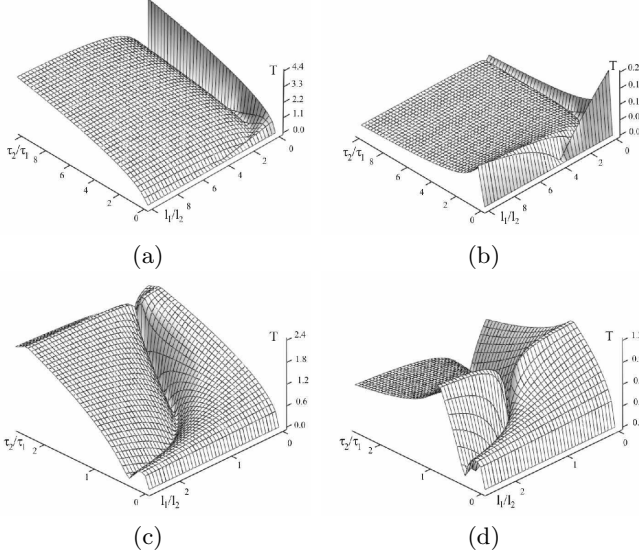


FIG. 4: The view of the surface  $T$  in coordinates  $(l_1/l_2, \tau_2/\tau_1)$  for  $\beta = 2$  and different values of  $u_1$  ( $u_1 = 0.1$  - (a),  $u_1 = 5.0$  - (b),  $u_1 = 1.25$  - (c),  $u_1 = 1.5$  - (d))

$$T = 2\sqrt{\beta} / \left[ \left| (1 - \bar{u}_1^2) \frac{l_1^2 \tau_2 + l_2^2 \tau_1}{l_1^2 \tau_2 - l_2^2 \tau_1} \right| - (1 - \bar{u}_1^2) \tau_2/\tau_1 + 1 \right]. \quad (15)$$

The plot of these surfaces, as a function of  $l_1/l_2$  and  $\tau_2/\tau_1$ , are presented in plots 3 (a-d) for different values of  $\bar{u}_1$ . We can see that in Fig. (a) and (b) the maximum value of  $T$  is reached at the boundary and  $l_1/l_2 \ll 1$  (Fig. 3a) and  $\tau_2/\tau_1 \ll 1$  (Fig. 3b). For figure. 3 c,d the optimal instability conditions are reached at certain combination of the parameters  $l_1/l_2$  and  $\tau_1/\tau_2$  and we can expect inhomogeneous oscillations at different relationships of  $l_1/l_2$  and  $\tau_1/\tau_2$ .

We expect the oscillatory structures to emerge if at given values of  $\bar{u}_1$ ,  $l_1/l_2$  and  $\tau_1/\tau_2$ , the fractional derivative index  $\alpha$  is greater than the one represented on the surface and less than the one needed for Hopf bifurcations for  $k = 0$ . This means that only the perturbations with these wave numbers are unstable, and they are unstable for oscillatory fluctuations. This situation is qualitatively different from the integer RD system whether either Turing ( $k \neq 0$ ) or Hopf bifurcation ( $k = 0$ ) takes place, and this depends on which condition is easier to realize. Thus, in the system under consideration, we can choose the parameter when we don't have Turing and Hopf bifurcations (for  $k = 0$ ) at all. Nevertheless, we obtain that conditions for Hopf bifurcation can be realized for a nonhomogeneous wave number. As it is seen from the figure, there are conditions where only instability according to non-homogeneous wave numbers holds. As a result, perturbations with  $k = 0$  relax to the homogenous state, and only the perturbations with a certain value of  $k$

become unstable and the system exhibits inhomogeneous oscillations.

## V. PATTERN FORMATION

The results of the numerical simulation of the fractional RDS (1) are presented on Fig. 4,5. From the pictures we can see that in such system we obtain a rich scenario of pattern formation: standard homogeneous oscillations, Turing stable structures, interacting inhomogeneous structures and inhomogeneous oscillatory structures. We have obtained that the ratio of characteristic times and the order of fractional derivative qualitatively transform pattern formation dynamics: homogeneous oscillations in the first limiting case and stationary dissipative structures in the second one [10]. Here we show that the change in any parameter which qualitatively changes the eigenvalues of the linearized system can change the system dynamics. Spatiotemporal dynamics of the FRD system can mainly be determined by the maximum eigenvalues for the corresponding modes. In Fig. 4a,b we can see stationary dissipative structures as a result of formation of the unstable mode presented in Fig. 2b(iv) for  $\alpha < 1$ . External parameter  $A$  determines the intersection point and the slope of the isoclines in this point and the power for each particular mode at this parameter. In particular, for  $A = 0.25$  nullclines intersect at the point where maximum value has eigenvalue with  $k = 2$ , which is responsible for Turing bifurcation with stationary structures. For  $A=0.5$  (Fig. 2b(iv)) nullclines intersect at the point where Hopf bifurcation takes place. The characteristic feature for these two limit cases is the instantaneous formation of either dissipative structures or homogeneous oscillations. Increasing influence of Hopf bifurcation when the Turing one is dominant, or increasing Turing bifurcation when Hopf is dominant, leads to more complicated transient dynamics (Fig. 4c,d). When conditions of these two instabilities practically coincide, we can obtain either oscillatory inhomogeneous structures or modulated homogeneous oscillations (Fig. 4e,f). Moreover, at parameters, when the real part of eigenvalues is close to zero, small variation of  $\alpha$  changes the type of bifurcation. This trend is typical for any  $\alpha \leq 1$ . For  $\alpha > 1$  the structure formation can be much more complicated.

Let us consider the bifurcation diagram presented in Fig. 1b,d. It was already noted that the region inside the curve is unstable for wave numbers  $k = 0$  and outside - it is stable. From the viewpoint of homogeneous oscillations, the system is stable near  $\bar{u}_1 = 0$ . However, if we have  $l_1 \ll l_2$ , the system becomes unstable according to Turing instability. As a result, we expect the formation of stationary inhomogeneous structures. In fact, at the beginning, only inhomogeneous fluctuations grow in amplitude and lead to inhomogeneous pattern formation. At the same time, at the dynamics of structure formation, the amplitude of the structures increases, and at

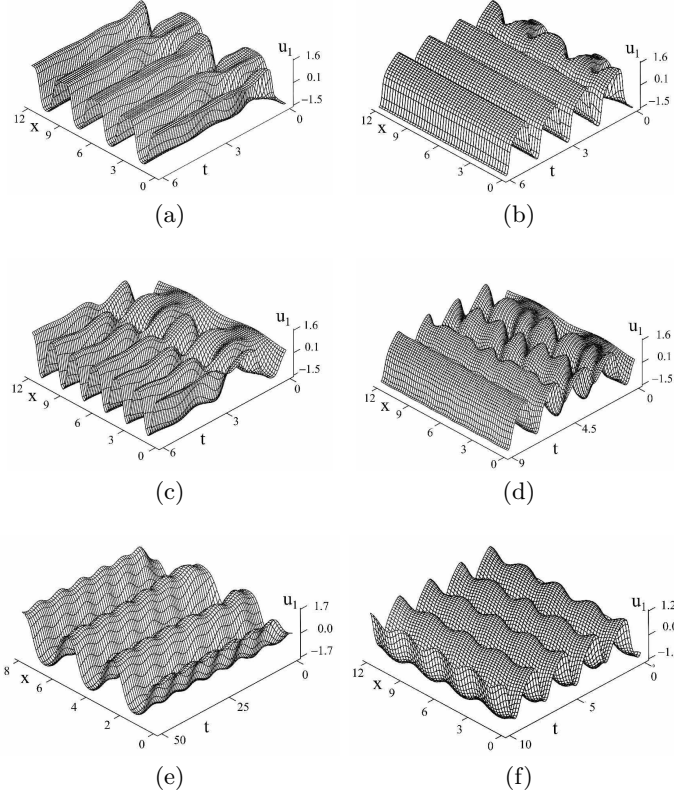


FIG. 5: Dynamics of pattern formation for  $u_1$  variable. The results of computer simulations of the system at parameters:  $\alpha = 0.8$ ,  $A = -0.25$ ,  $\beta = 2.1$ ,  $l_1 = 0.025$ ,  $l_2 = 1$ ,  $\tau_1/\tau_2 = 0.1$  – (a);  $\alpha = 0.8$ ,  $A = -0.55$ ,  $\beta = 2.1$ ,  $l_1 = 0.025$ ,  $l_2 = 1$ ,  $\tau_1/\tau_2 = 0.1$  – (b);  $\alpha = 0.8$ ,  $A = -0.4$ ,  $\beta = 2.1$ ,  $l_1 = 0.025$ ,  $l_2 = 1$ ,  $\tau_1/\tau_2 = 0.1$  – (c);  $\alpha = 0.8$ ,  $A = -0.45$ ,  $\beta = 2.1$ ,  $l_1 = 0.025$ ,  $l_2 = 1$ ,  $\tau_1/\tau_2 = 0.1$  – (d);  $\alpha = 1.6$ ,  $A = -0.01$ ,  $\beta = 1.05$ ,  $l_1 = 0.05$ ,  $l_2 = 1$ ,  $\tau_1/\tau_2 = 1.45$  – (e);  $\alpha = 0.7$ ,  $A = -0.3$ ,  $\beta = 2.1$ ,  $l_1 = 0.05$ ,  $l_2 = 1$ ,  $\tau_1/\tau_2 = 0.2$  – (f);

maximum and minimum amplitude, the structures fall into the domain where the homogenous structures are unstable. As result, we obtain complex interaction of Turing and Hopf bifurcations (Fig. 5a,b).

Inhomogeneous oscillatory structures are presented on pictures (Fig. 5 c,d)). Due to different evolution pattern for two variables, the activator variable  $u_1$  is presented in the left column and the inhibitor one  $u_2$  is presented on the right column. Such structures are obtained at eigenvalues with negative real part when the intersection of the null-cline for activator variable is located on the decreasing part of null cline  $u_2(u_1)$ . The corresponding eigenvalues for this situation are presented in Fig. 2b(v). From the eigenvalue plots (Fig. 2) we can see corresponding separated domains where inhomogeneous oscillatory modes with  $k = 2$  are unstable. Successive increase of the fractional derivative index will increase the amplitude of the presented in Fig. 5a,b inhomogeneous oscillation. As a result, inhomogeneous oscillatory structures of large

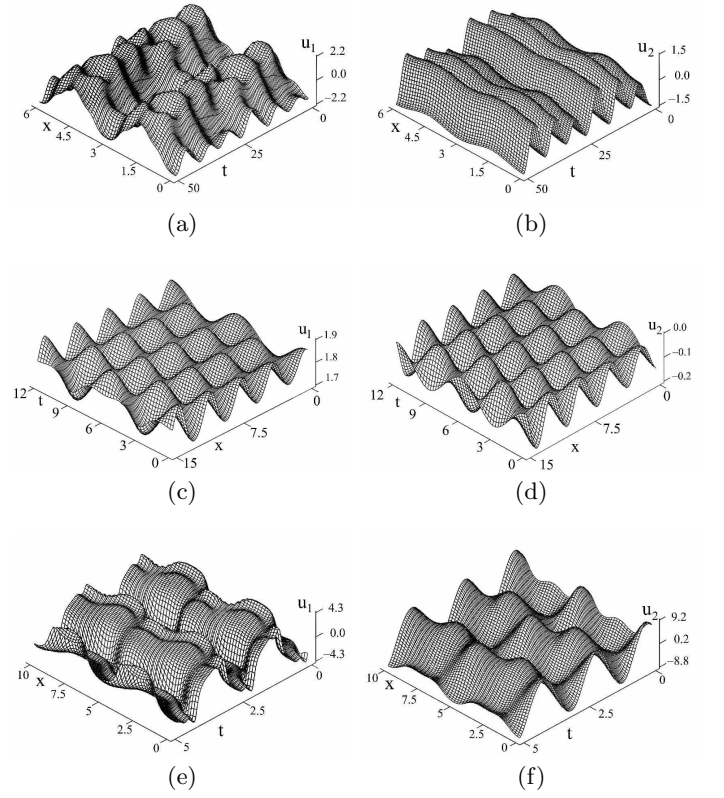


FIG. 6: Dynamics of pattern formation for  $u_1$  (left column) and  $u_2$  (right column) variables. The results of computer simulations of the systems at parameters:  $A = -0.01$ ,  $\alpha = 1.8$ ,  $\beta = 1.01$ ,  $l_1 = 0.02$ ,  $l_2 = 1$ ,  $\tau_1/\tau_2 = 3.5$  – (a-b);  $A = 1.95$ ,  $\alpha = 1.82$ ,  $\beta = 1.01$ ,  $l_1 = 0.1$ ,  $l_2 = 1$ ,  $\tau_1/\tau_2 = 0.6$  – (c-d);  $A = -0.01$ ,  $\alpha = 1.75$ ,  $\beta = 10$ ,  $l_1 = 0.05$ ,  $l_2 = 1$ ,  $\tau_1/\tau_2 = 0.05$  – (e-f);

amplitude are realized in the system.

Another type of oscillatory structures with a little bit more complicated dynamics are presented in Fig. 5e,f for  $\beta = 10$ ,  $\tau_1 \ll \tau_2$  and  $\alpha \lesssim 2$ . As in the case considered above we have inhomogeneous oscillatory structures the surface of which in the region of slow motion oscillates with fast frequency  $1/\tau_1$ . Such behaviors are due to oscillatory property of the activator system at  $\alpha$  approaching the value of 2.

## VI. CONCLUSION

We have shown a complex spatio-temporal pattern formation in simple FRD system and compared these results with standard one. The fractional derivative index plays a crucial role in this pattern formation because conditions of time bifurcations depend substantially on its value. By eigenvalue analysis we have studied instability conditions for  $k = 0$ , and  $k \neq 0$  for different values of external parameter  $\mathcal{A}$  (the same as  $\bar{u}_1$ ). Nonlinear solutions show

that dynamics of the system is determined by most unstable modes. When linear increments are comparable, we have an interplay between Hopf and Turing modes leading to more complex dynamics.

When a fractional derivative index is changed from 0 to 1, the large-amplitude structures are stationary if a limit cycle is damped at  $\tau_1 \simeq \tau_2$ . Oscillatory structures at these values of fractional derivative index can be realized only at  $\tau_1 << \tau_2$ .

When a fractional derivative index is changed from 1 to 2, the large-amplitude structures have more complex dynamics. Moreover, the spatiotemporal structures are observed even at  $\tau_1 \gg \tau_2$ . Complex structures are observed in the region, when the bifurcation parameter leads to Turing and Hopf instabilities, as well as in the regions where these instabilities are damped. The system moves to large amplitude limit cycle with further change in the fractional derivative index.

- 
- [1] Nicolis, G., Prigogine, I., 1997, *Self-organization in Non-equilibrium Systems*, Wiley, New York.
  - [2] Cross, M. C. and Hohenberg, P. C., 1993, "Pattern formation outside of equilibrium", *Rev. Mod. Phys.*, Vol. **65**, pp. 851-1112.
  - [3] Kerner, B.S., Osipov, V.V., 1994, *Autosolitons*, Kluwer, Dordrecht.
  - [4] Henry, B.I., Langlands, T.A.M. and Wearne, S.L., 2005, "Turing pattern formation in fractional activator-inhibitor systems", *Phys. Rev. E*, Vol. **72**, 026101(14 p.)
  - [5] Langlands, T.A.M., Henry, B.I. and Wearne, S.L., 2007, "Turing pattern formation with fractional diffusion and fractional reactions", *J. Phys.: Condens. Matter*, Vol. **19**, 065115 (20 p.)
  - [6] Hernandez, D., Varea, C. and Barrio, R. A., 2009, "Dynamics of reaction-diffusion systems in a subdiffusive regime", *Phys. Rev. E*, Vol. **79**, 026109 (10 p.)
  - [7] Gafiychuk, V., Datsko, B., 2006, "Pattern formation in a fractional reaction-diffusion system", *Physica A*, Vol. **365**, 300-306.
  - [8] Gafiychuk, V., Datsko, B., 2007, "Stability analysis and oscillatory structures in time-fractional reaction-diffusion systems", *Phys. Rev. E*, Vol. **75**, 055201(4 p.) (R)
  - [9] Gafiychuk, V. and Datsko, B., 2008, "Inhomogeneous oscillatory structures in fractional reaction-diffusion systems", *Physics Letters A*, Vol. **372**, pp.619-622.
  - [10] Gafiychuk, V., Datsko, B., Meleshko, V., 2008, "Mathematical modeling of time fractional reaction-diffusion systems", *J. Comp. Appl. Math.*, Vol. **220**, pp. 215-225.
  - [11] Golovin, A. A., Matkovsky, B. J., Volpert, V. A., 2008, "Turing pattern formation in the brusselator model with superdiffusion", *SIAM J. Appl. Math.*, Vol. **60**, pp. 251-272.
  - [12] Nec, Y., Nepomnyashchy, A. A. and Golovin, A. A., 2008, "Oscillatory instability in super-diffusive reaction-diffusion systems: Fractional amplitude and phase diffusion equations", *EPL*, Vol. **82**, 58003 (6 p.).
  - [13] Zaslavsky, G.M., 2002, "Chaos, fractional kinetics, and anomalous transport", *Phys. Rep.*, Vol. **371**, pp. 461-580.
  - [14] Metzler, R. and Klafter, J., 2000, "The random walk's guide to anomalous diffusion: a fractional dynamics approach", *Phys. Rep.*, Vol. **339**, pp. 1-77.
  - [15] Agrawal, O. P., Tenreiro Machado, J. A., Sabatier, J., 2007, *Advances in Fractional Calculus : Theoretical Developments and Applications in Physics and Engineering*, Elsevier.
  - [16] Kilbas, A. A., Srivastava, H. M., Trujillo, J. J., 2006, *Theory and Applications of Fractional Differential Equations*, Elsevier.
  - [17] Uchaikin, V. V., 2008, *Fractional derivative method*, Artishok (in Russian).
  - [18] Podlubny, I., 1999, *Fractional Differential Equations*, Academic Press.
  - [19] Samko, S.G., Kilbas, A. A. and Marichev, O. I., 1993, *Fractional Integrals and Derivatives: Theory and Applications*, Gordon and Breach, Newark, N.J.
  - [20] R. FitzHugh, *Biological Engineering*, McGraw-Hill (1969), 1-85.